Water-Quality Principles
QW1022–TEL

Lesson 13—Interpretive Methods

Source: Alley, W.M., ed., 1993, Regional ground-water quality: New York, Van Nostrand Reinhold , p. 42–48 and 199–205. Reproduced with permission of John Wiley & Sons, Inc.

U.S. Department of the Interior
U.S. Geological Survey

from the pores and relatively dilute storm-derived water associated with recent rainfall events.

Tracing methods and water chemistry are widely used for studying karst aquifers. Extensive tracer studies combined with field work to locate points of recharge and discharge have been used to estimate the recharge areas of springs, rates of ground-water movement, and the water balance of aquifers. Variations in parameters such as temperature, hardness, Ca–Mg ratios, Ca and Mg saturation indices, and carbon-14 have been used to describe sources and rates of ground-water movement, differentiate rapid and slow karst ground-water components, and compare spring-flow characteristics in different regions.

Rapid transport of contaminants within karst aquifers and to springs has been observed in many locations. Because of the rapid movement of water in many karst aquifers, water-quality problems that may be localized in other aquifer systems can become regional in nature in karst systems. Unique aspects of karst aquifers and special considerations for ground-water monitoring are reviewed in Chapter 19.

USES OF GEOCHEMICAL DATA IN REGIONAL CONCEPTUALIZATIONS

The kinds of ions in solution and their concentrations result from chemical processes relating to the lithology and hydrologic flow pattern of a particular hydrologic system. Thus, an analysis of geochemical data, both existing and newly collected data, is useful in developing a regional hydrogeologic framework. A few commonly used approaches for the display and analysis of geochemical data will be briefly reviewed with examples of their applications to regional interpretation of ground-water quality. The related topics of geochemical models and environmental isotopes are covered separately in Chapters 9 to 11. Descriptions of ground-water quality associated with different lithologies are given by Freeze and Cherry (1979), Matthess (1982), and Hem (1985).

Map and Graphical Displays

Simple Map Displays

One of the simplest means of displaying geochemical data is a dot map of the quality of ground water prepared by entering numbers or symbols at well and spring locations to represent concentrations of constituents. Through shading, color coding, or by their size, dots displayed at the sampled locations can be used to indicate different concentration ranges. In general, dot maps have limited ability to illustrate spatial patterns in water quality. If many analyses exist, and the ground-water body exhibits relatively distinct patterns in water quality, then maps showing isopleths of chemical characteristics within certain formations can be constructed. Care must be exercised in all types of map presentation to consider possible depth variations in ground-water quality.

Stiff Patterns

A common method of presentation of geochemical data is the Stiff (1951) pattern. A polygonal shape is created from the plotting of chemical values along horizontal axes which are separated from each other by

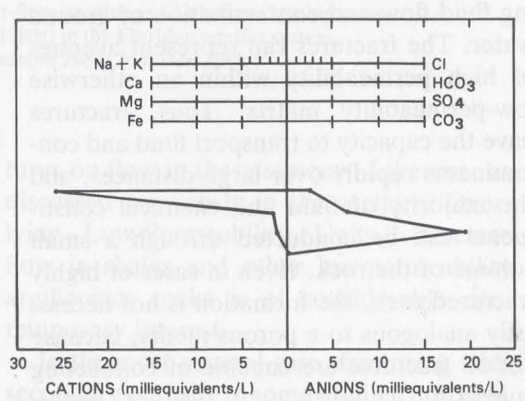

FIGURE 2-10. Example of Stiff pattern.

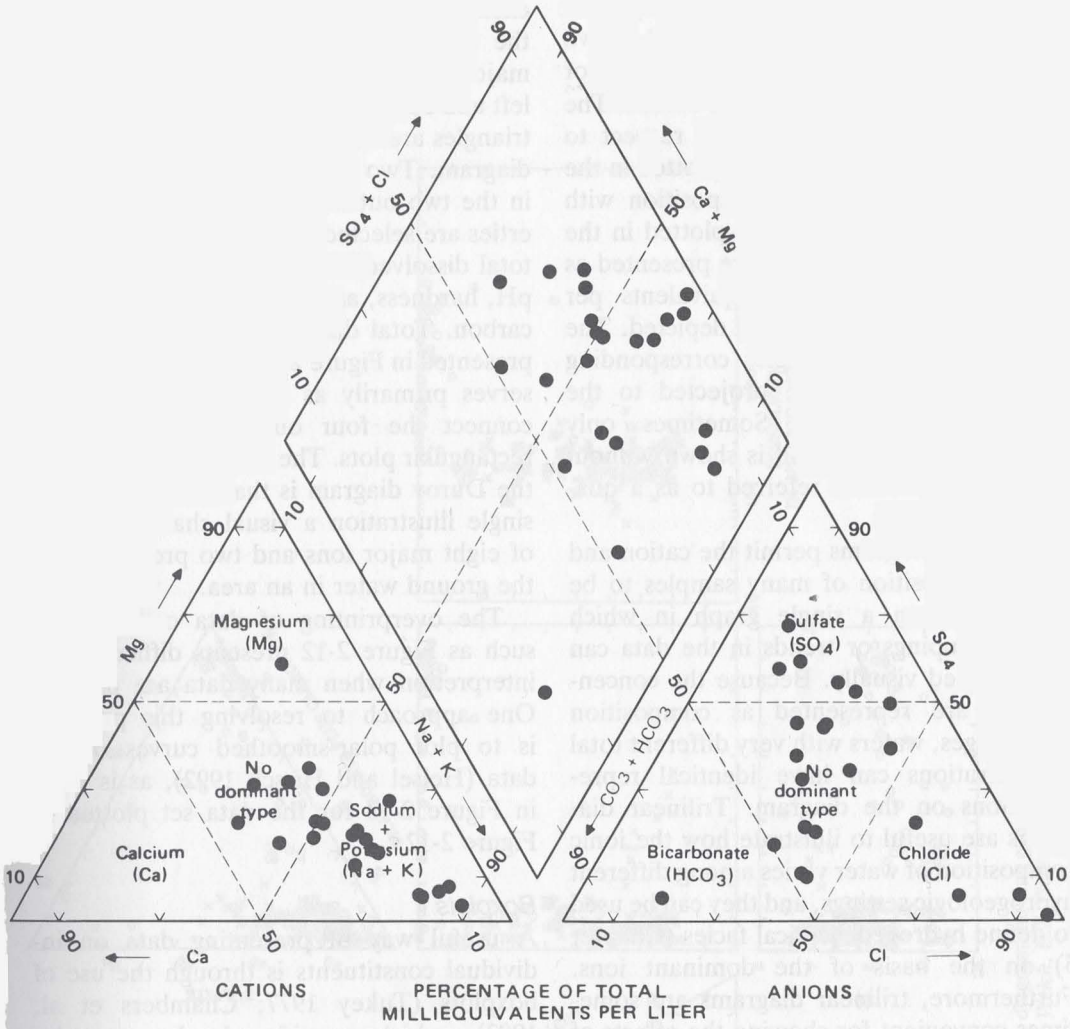

FIGURE 2-11. Example of a trilinear diagram showing chemical composition of ground water in confined zone in northwestern part of San Joaquin Valley, California. (*After Dubrovsky et al. 1991.*)

equal distances and are divided by a vertical center line. Cations are plotted in milliequivalents per liter on one side of the vertical axis and anions on the opposite side. An example Stiff pattern is shown in Figure 2-10. The use of the lower horizontal bar with iron and carbonate is optional, because the concentrations of these two constituents can be close to zero. Sometimes other constituents, such as nitrate, are shown on the lower horizontal bar. Stiff patterns facilitate rapid comparisons among water from different sources as a result of their distinctive graphic shapes. They are useful for illustrating chemical composition in hydrogeologic cross sections and as a symbol on maps. They are not, however, well suited for graphical presentation of large numbers of analyses.

Trilinear Diagrams

A commonly used method of graphical presentation is the trilinear diagram (Hill 1940; Piper 1944). Several variants of the

trilinear diagram exist; a frequently used version is shown in Figure 2-11. Two triangles are displayed: one for major cations and the other for major anions. The composition of the water with respect to cations is indicated by a point plotted in the cation triangle, and the composition with respect to anions by a point plotted in the anion triangle. The values are presented as percentages of total milliequivalents per liter of the cations or anions depicted. The points in the two triangles corresponding to a single sample are projected to the diamond-shaped field. Sometimes only the diamond-shaped field is shown without the triangles, and is referred to as a quadrilinear diagram.

Trilinear diagrams permit the cation and anion composition of many samples to be represented on a single graph in which major groupings or trends in the data can be discerned visually. Because the concentrations are represented as composition percentages, waters with very different total concentrations can have identical representations on the diagram. Trilinear diagrams are useful to illustrate how the ionic composition of water varies among different hydrogeologic settings, and they can be used to define hydrogeochemical facies (Chapter 5) on the basis of the dominant ions. Furthermore, trilinear diagrams are sometimes convenient for showing the effects of the mixing of two waters from different sources; the mixture of two different waters will plot on the straight line joining the two points, if the ions are not added or removed from solution by processes such as ion exchange, precipitation, or solution of salts.

Durov Diagrams

The Durov diagram (Chilingar 1956; Zaporozec 1972) is a method of presentation similar to the trilinear diagram. An example is shown in Figure 2-12 for ground water in two parts of the Carson River basin in eastern Nevada and western California.

The Durov diagram consists of five fields, two triangular and three rectangular. Each chemical analysis is plotted as five points on the diagram. The relative percentages of major cations and anions are shown on the left and upper triangles, respectively. These triangles are similar to those of the trilinear diagram. Two other properties are plotted in the two outside rectangles. These properties are selected from possibilities such as total dissolved solids, specific conductance, pH, hardness, and total dissolved inorganic carbon. Total dissolved solids and pH are presented in Figure 2-12. The central square serves primarily as a transitional area to connect the four outside triangular and rectangular plots. The primary advantage of the Durov diagram is that it provides on a single illustration a visual characterization of eight major ions and two properties for the ground water in an area.

The overprinting of data on diagrams such as Figure 2-12 presents difficulties in interpretion when many data are plotted. One approach to resolving this problem is to plot polar-smoothed curves of the data (Helsel and Hirsch 1992), as is done in Figure 2-13 for the data set plotted in Figure 2-12.

Boxplots

A useful way of presenting data on individual constituents is through the use of boxplots (Tukey 1977; Chambers et al. 1983), which provide visual summaries of the statistical distribution and key statistical characteristics of a data set. Boxplots commonly are placed side-by-side to compare and contrast groups of data. In this way, they are useful for comparing individual water-quality constituents among different settings.

Boxplots shown in Figure 2-14 show statistical distributions of nitrate and boron in shallow ground water underlying five land-use types on Long Island. The box part of the boxplot is drawn from the 25th percentile (lower quartile) to the 75th percentile (upper quartile) of the data, and a line is drawn across the box at the median value. The box illustrates several key

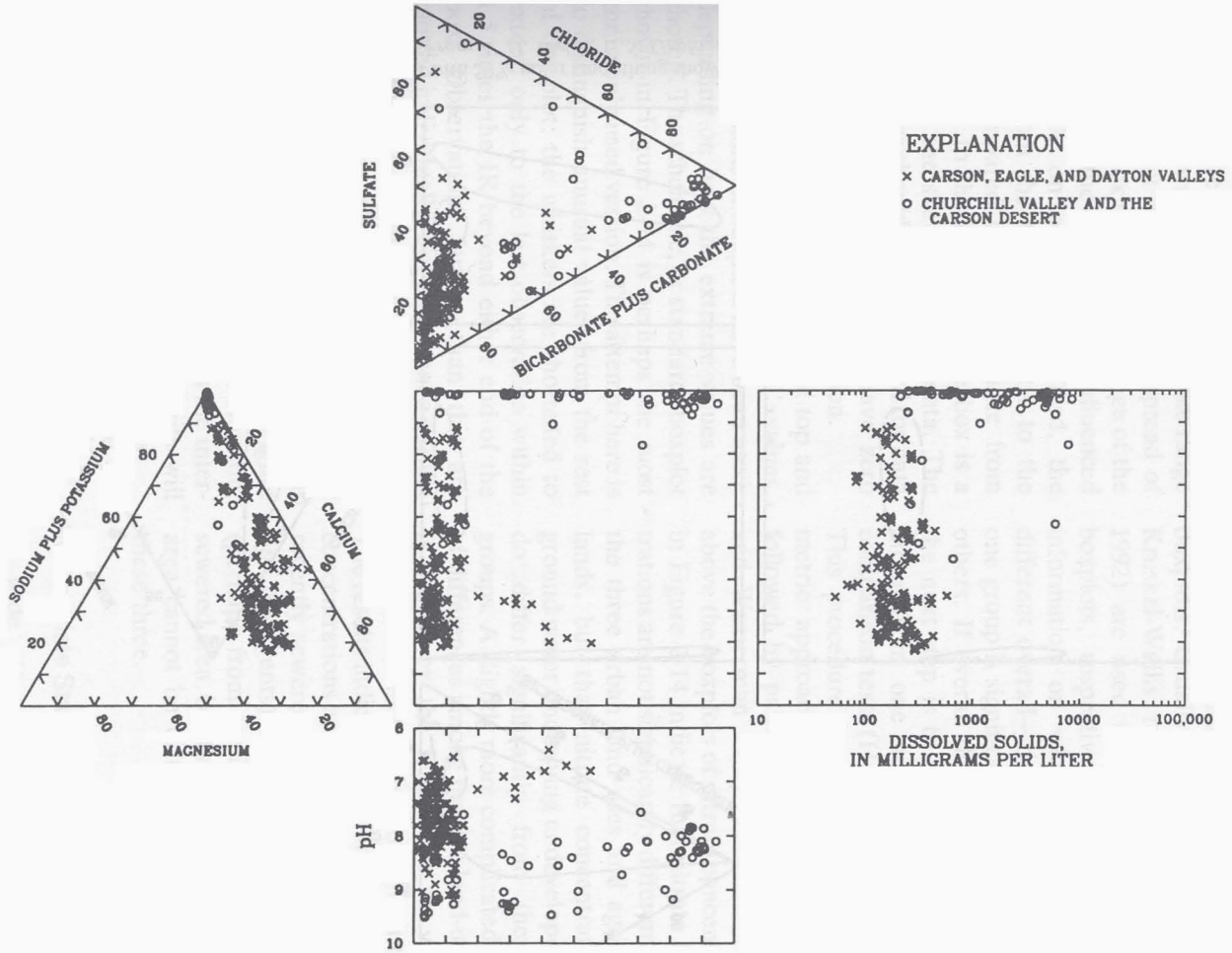

FIGURE 2-12. Example of Durov diagram showing general chemical character of principal aquifers in Carson River basin, Nevada and California. (*From A. H. Welch, U.S. Geological Survey, written commun., 1991.*)

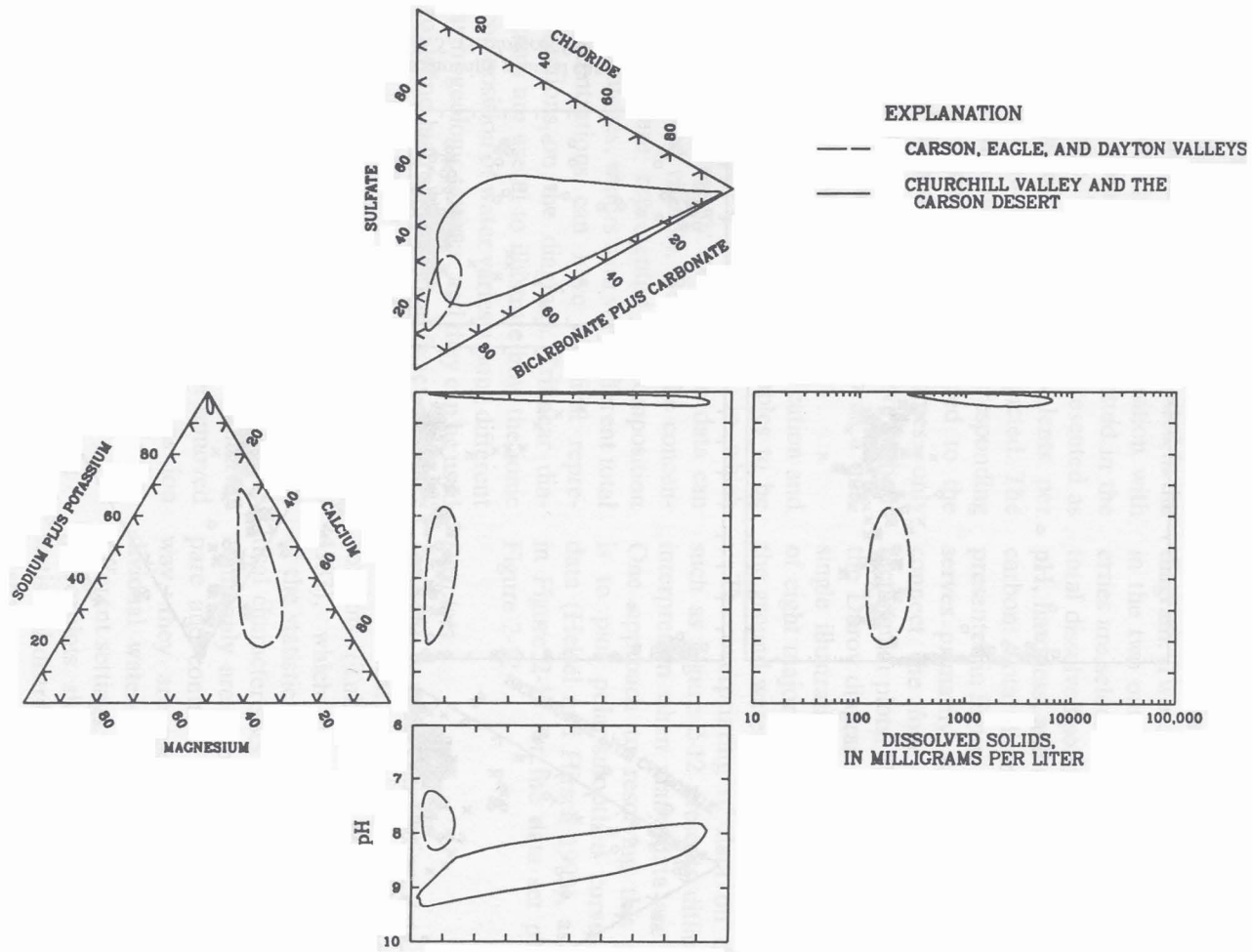

FIGURE 2-13. Example of Durov diagram with 50% polar smoothing showing general chemical character of principal aquifers in Carson River basin, Nevada and California. (*From A. H. Welch, U.S. Geological Survey, written commun., 1991.*)

features of the distribution of the data. First, the sample median is a robust measure of the central tendency of the data that is not influenced by extreme values. Second, the difference between the top and bottom of the box, known as the interquartile range (IR), is a robust measure of the spread of the data. The box measures the range of the central 50% of the data and is not influenced by the 25% on either end. Third, the distance from the top of the box to the median compared with the distance from the median to the bottom of the box is a measure of the skewness of the data. The two distances should be about equal for data derived from distributions that have zero skew such as the normal distribution.

"Whiskers" are drawn from the top and bottom of the box to "extreme" values. Several variants of boxplots have been used, depending on how the extreme values are chosen. The schematic, or standard, boxplot shown in Figure 2-14 is perhaps the most commonly used version. The attempt here is to distinguish unusual values from the rest of the plot; the whiskers are shortened to extend only to the last observation within 1.5 times the IR beyond either end of the box. Observations farther than this are plotted individually. For data from a normal distribution, these values will occur less than 1% of the time. Observations farther than 3 times the IR from either end of the box are additionally distinguished by a different symbol (e.g., a square is used in Figure 2-14). For data from a normal distribution, values more extreme than 3 times the interquartile range beyond the box limits will occur fewer than once in 300,000 times.

Other versions of the boxplot are the "simple" boxplot in which the whiskers are simply drawn from the ends of the box to the maximum and minimum data values, and a version in which the whiskers are drawn only to the 10th and 90th percentiles of the data set; the largest 10% and smallest 10% of the data are not shown. This latter type should be used only when the extreme 20% of the data are not of interest. Features sometimes added to boxplots include confidence limits about the sample median and key limits such as water-quality standards.

Statistical tests of differences among the data groups commonly are reported with the boxplots. Usually, the Mann-Whitney and Kruskal-Wallis tests (Helsel and Hirsch 1992) are used in cases of two or more boxplots, respectively. These tests yield information on whether the groups are different overall—that is, whether at least one group is significantly different from the others. If overall differences are detected, the next step is to ascertain which groups differ from one another using multiple-comparison tests (Helsel and Hirsch 1992). This procedure is analogous to the parametric approach of analysis of variance followed by pairwise-contrast tests (Neter and Wasserman 1974). The letters shown above the boxplots of nitrate concentrations in Figure 2-14 indicate that nitrate concentrations are not significantly different among the three urban land uses and agricultural lands, but that nitrate concentrations in ground water underlying undeveloped lands do differ significantly from these four groups. A slightly more complicated pattern of differences among the five land-use types is shown by the letters for the multiple comparison tests of boron concentrations. The results indicate, for example, that boron concentrations are significantly higher in the recently sewered area (perhaps from laundry detergents) and the agricultural area (perhaps from fertilizers) than in the unsewered area, but that the longterm sewered area cannot be distinguished from any of these three.

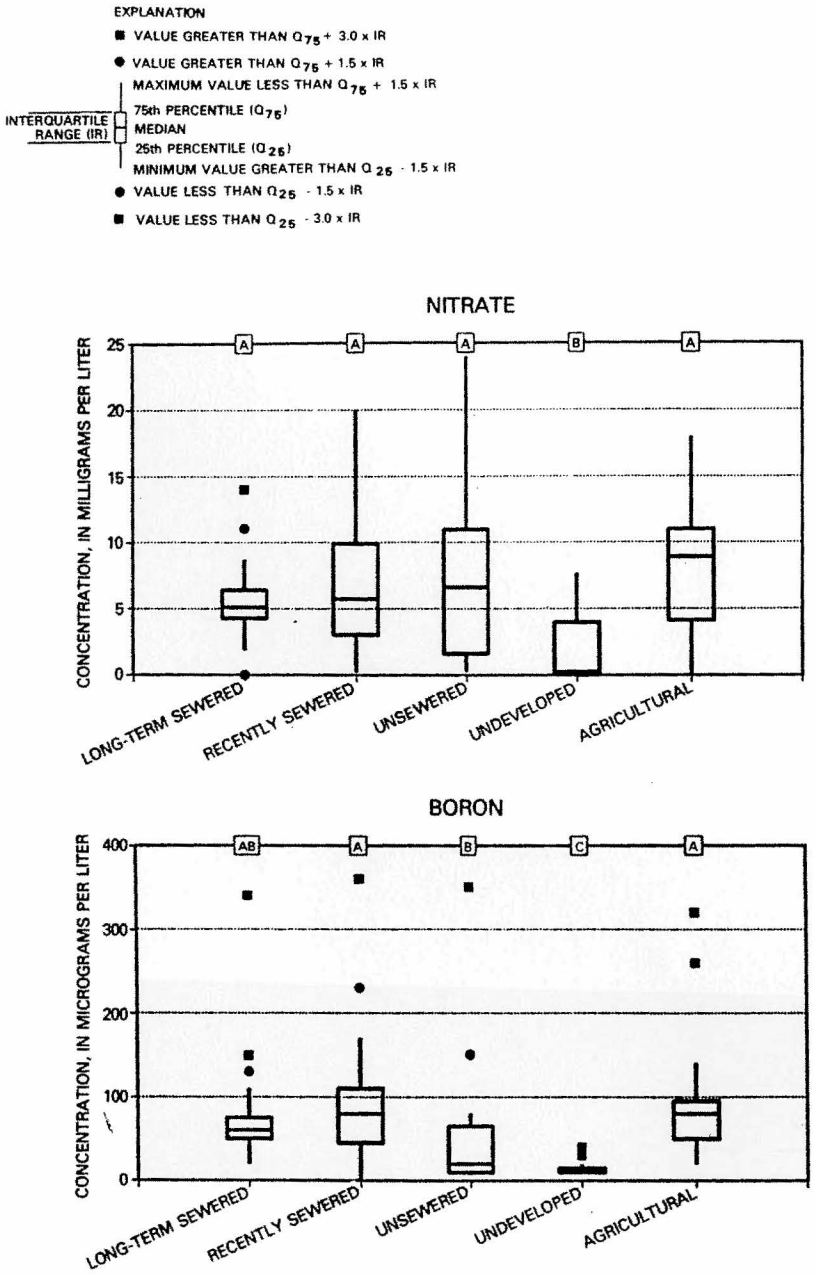

FIGURE 2-14. Boxplots of nitrate and boron in ground water underlying five land-use types on Long Island, New York. Letters above boxplots indicate results of multiple comparison tests (groups of data with common letters do not differ statistically). Sample sizes are 20 for first three groups and 15 for last two groups. (*After Eckhardt, Siwiec, and Cauller 1989.*)

9

Geochemical Models

D. L. Parkhurst and L. N. Plummer

INTRODUCTION

Geochemical models are tools that aid in the interpretation of geochemical reactions. Many different geochemical models have been applied to a wide range of surface- and ground-water problems. This chapter focuses on the application of geochemical models to regional ground-water systems. Here, the models can be used for a variety of purposes, including determination of the prevailing geochemical reactions, quantification of the extent to which these reactions occur, prediction of the fate of inorganic contaminants, and estimation of the direction and rates of ground-water flow. Plummer (1984) divided geochemical modeling into two general approaches: (1) inverse modeling, which uses observed ground-water compositions to deduce geochemical reactions; and (2) forward modeling, which uses hypothesized geochemical reactions to predict ground-water compositions. Inverse modeling produces quantitative geochemical reactions that describe the chemical evolution in a ground-water system, whereas forward modeling begins at some starting composition and simulates the chemical evolution of ground water in response to sets of specified reactions. In regional ground-water studies where chemical and isotopic data are available, inverse modeling is the most efficient approach because its results always reproduce the chemistry of the available samples. The forward approach is appropriate for systems or chemical constituents as yet unstudied, where the goal is to predict the chemical composition of ground water in the absence of chemical data. The forward approach also is uniquely capable of simulating advection, dispersion, and spatial and temporal distributions of minerals and ground-water composition. In this chapter, the techniques involved in inverse and forward modeling are presented, and the utility and deficiencies of each approach are discussed. Examples of each type of modeling are presented to illustrate the interpretation of model results.

INVERSE MODELING

The purpose of inverse modeling is to determine net chemical reactions that quantitatively account for the chemical and isotopic composition of ground-water samples and are consistent with known thermodynamic constraints and mineralogic observations. The pioneering work in this approach is

by Garrels and Mackenzie (1967), who quantified the amounts of specific silicate-weathering reactions that were necessary to account for the differences in chemical concentrations between two springs in the Sierra Nevadas. For ground water, the modeling typically is applied to water samples from two wells that are assumed to be on a single flow path in order to determine the net chemical reaction that has occurred between the two wells. The inverse modeling described here is a combination of speciation modeling and mass-balance modeling, with special reference to the programs WATEQF (Plummer, Jones, and Truesdell 1976) and NETPATH (Plummer, Prestemon, and Parkhurst 1991). Speciation modeling, isotopic data, and petrographic observations provide constraints on whether plausible reactant phases are dissolving, are precipitating, or are inert. Mass-balance modeling produces quantitative geochemical reactions that reproduce the compositions of the samples and are consistent with any constraints on the reactant phases.

Speciation Modeling

Speciation models calculate thermodynamic properties of aqueous solutions, including the molalities and activities of aqueous species and saturation indices of minerals. Two main approaches are currently used to calculate these properties: the ion-association approach and the specific-interaction approach. The ion-association approach attempts to account for much of the nonideality of aqueous solutions by ion association, that is, the formation of complexes from the hydrated individual ions in solution. An example of a complexation reaction is given in Eq. 9-1.

$$Ca^{2+} + SO_4^{2-} \rightarrow CaSO_4^0 \qquad (9\text{-}1)$$

The complexes have mass-action equations that relate the activities of the aqueous species; the mass-action equation for this example is

$$K_{CaSO_4^0} = \frac{[CaSO_4^0]}{[Ca^{2+}][SO_4^{2-}]} \qquad (9\text{-}2)$$

where $K_{CaSO_4^0}$ is the stability constant, which is a function of temperature and pressure, and brackets indicate activity. Activities are related to molality (moles per kilogram of water) by

$$[i] = \gamma_i(i) \qquad (9\text{-}3)$$

where (i) is the molality of species i and γ_i is the activity coefficient. Activity coefficients of individual ions and complexes are usually estimated using extensions of the Debye-Hückel theory.

The advantages of the ion-association approach are that it is relatively easy to modify the model to include new species and new elements. Activity coefficients for species can be estimated using a form of the Debye-Hückel equation that only requires the electrical charge of the species to be known. Extensive literature exists that identifies complexation reactions and estimates the stability constants. The major deficiencies of the models are (1) the original Debye-Hückel theory only applies at very low ionic strengths (less than 0.01), and extensions of the theory are only applicable to selected solution compositions (generally sodium chloride solutions) of moderate ionic strengths approaching seawater concentrations (ionic strength of 0.7); (2) in spite of their wide use, insufficient work has been done to ensure that the models are adequately reproducing experimental solution properties such as mineral solubilities and mean-activity coefficients; and (3) whereas attractive forces among aqueous species can be accounted for by ion association, there is no mechanism to account for repulsive forces in mixed electrolyte solutions. Some of the better known ion-association models are implemented in the codes MINTEQA2 (Allison, Brown, and Novo-Gradac 1990), GEOCHEM (Sposito and Mattigod 1980), EQ3 (Wolery 1979), WATEQF (Plummer,

Jones, and Truesdell 1976), WATEQ4F (Ball and Nordstrom 1991), and PHREEQE (Parkhurst, Thorstenson, and Plummer 1980). Characteristics of several of these and other speciation codes have been summarized by Mangold and Tsang (1991).

In contrast to the simple Debye-Hückel expressions for individual ion-activity coefficients in ion-association models, the specific-interaction approach uses a complex expansion of the Debye-Hückel expression to calculate mean-activity coefficients for chemical reactions. The expanded expression includes coefficients that account for specific interactions between every pair and triplet combination of aqueous species (see Pitzer 1979; and Harvie and Weare 1980). These mean-activity coefficients account for most of the nonideality of aqueous solutions; therefore, very few complexation reactions are included in the specific-interaction models. The advantage of this approach is that it is theoretically applicable to all mixed electrolyte solutions of any ionic strength. The specific-interaction parameters have been selected carefully to produce a consistent set of parameters and stability constants that reproduce the best available experimental data (Harvie and Weare 1980). The disadvantage of the approach is that it is currently applicable largely to elements that form strong electrolytes. In geologic contexts, the most notable omissions of elements in current implementations are aluminum and silicon as well as most trace elements. Currently, interaction parameters are available for at most a single valence state of redox elements, which means that these models are not applicable to many reactions that involve redox transitions. The specific-interaction approach has been implemented in the codes PHRQPITZ (Plummer et al. 1988) and EQ3/6 (Wolery et al. 1990), which can be used for speciation calculations.

The primary purpose of speciation modeling is to calculate mineral saturation indices, which are indicators of the saturation state of a mineral with respect to a given water composition. The saturation index is defined as

$$\mathrm{SI} = \log_{10}\left(\frac{\mathrm{IAP}}{K_{sp}}\right) \tag{9-4}$$

where SI is the saturation index, IAP is the ion-activity product as defined by a mass-action equation, and K_{sp} is the solubility-product constant for the mineral (also see Chapter 6). If the saturation index is less than zero, the mineral is undersaturated with respect to the solution and the mineral might dissolve. The saturation index only indicates what should happen thermodynamically; it does not indicate the rate at which the process will proceed. In many cases, a mineral having a saturation index less than zero may dissolve very slowly or not at all, depending on the kinetics of the reaction. A more definitive conclusion can be drawn if the mineral saturation index is less than zero; that is, the mineral cannot precipitate from the ground water. This conclusion is qualified only by the accuracy of the chemical analysis and the aqueous model, not by rates of reaction. By similar reasoning, if the saturation index is greater than zero, the mineral might precipitate but cannot dissolve. If the saturation index is close to zero, the mineral may not be reacting at all or may be reacting reversibly, in which case the mineral could be dissolving or precipitating.

Example of Speciation Modeling

An example of the interpretation of saturation indices is taken from a study of ground-water samples from the Madison aquifer in parts of Montana, Wyoming, and South Dakota (Plummer et al. 1990; Busby, Lee, and Hanshaw 1983). The Madison aquifer primarily is a limestone aquifer; calcite, dolomite, and anhydrite are the major minerals. Saturation indices for selected ground-water samples from this aquifer were calculated by using the speciation code WATEQF (Plummer, Jones, and Truesdell 1976). The saturation indices for calcite

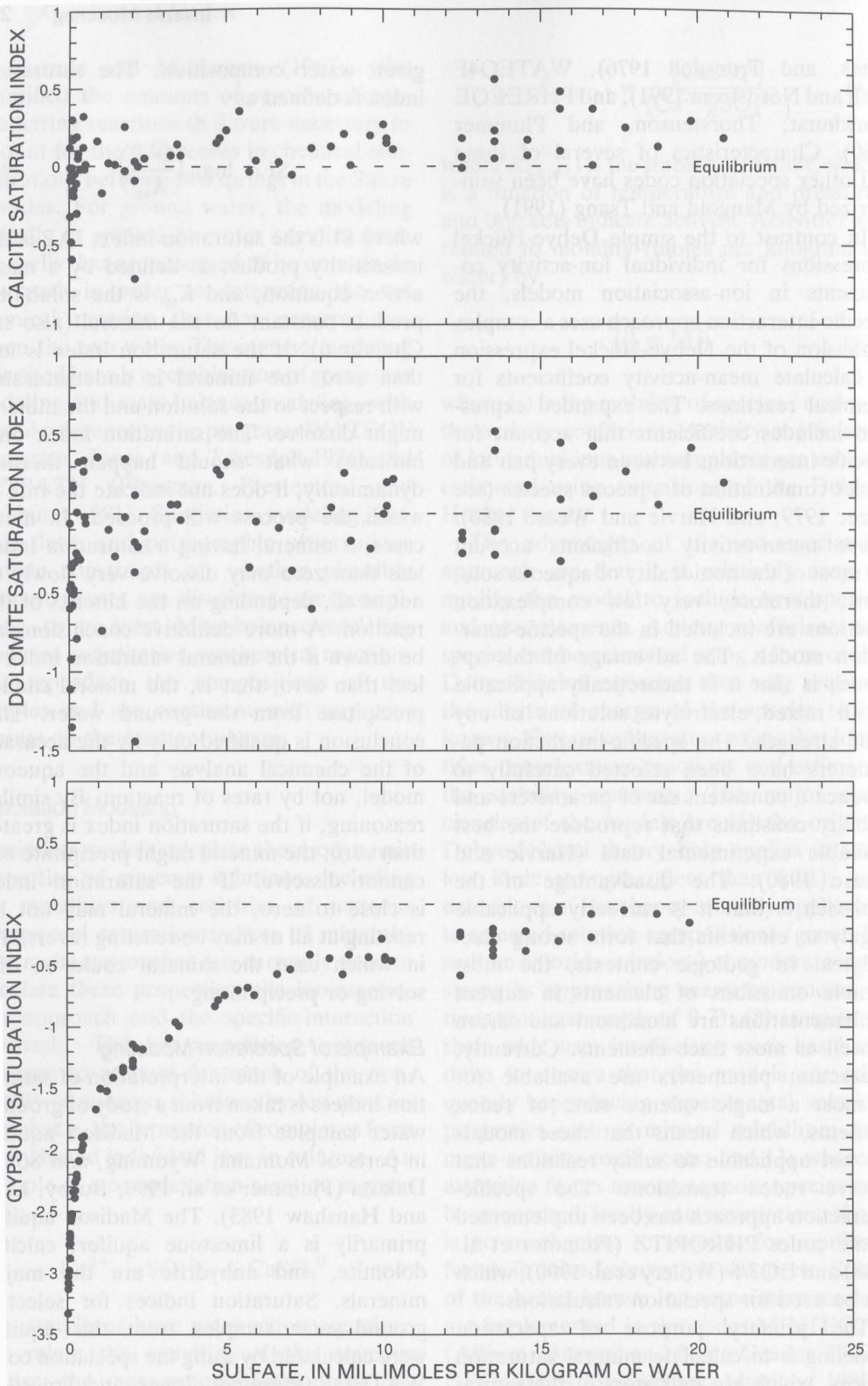

FIGURE 9-1. Comparison of calcite, dolomite, and gypsum saturation indices as a function of total dissolved-sulfate concentration for wells and springs in the Madison aquifer. (*From Plummer et al. 1990.*)

(Figure 9-1) are slightly greater than 0.0, which Plummer et al. (1990) attributed to supersaturation due to dedolomitization, pressure effects on the activities of species, variations in calcite stability caused by incorporation of sulfate into the mineral structure, or possibly CO_2 outgassing during the measurement of pH. Except in waters with very small sulfate concentrations, dolomite appears to be near saturation, if an uncertainty of ± 0.5 units is accepted. Plummer et al. (1990) used saturation indices for gypsum rather than anhydrite because the stability constant for gypsum is better known as a function of temperature. However, anhydrite should be slightly more stable than gypsum at the temperatures and salinities of ground water in this aquifer, so they conclude that waters that have more than about 14 mmol/kg H_2O sulfate are in equilibrium with anhydrite. Thus, the saturation indices indicate that anhydrite is dissolving, dolomite is reacting reversibly, and calcite appears to be precipitating in the Madison aquifer. This is consistent with the process of dedolomitization, in which anhydrite dissolves and causes the dissolution of dolomite and the precipitation of calcite.

Plummer et al. (1990) also noted that the saturation indices for celestite ($SrSO_4$) are very similar to those for gypsum in that they indicate saturation at large sulfate concentrations. Strontianite ($SrCO_3$) saturation indices also are found to be nearly constant, though at a saturation index of about -1.0. Plummer et al. (1990) showed that the constant, negative saturation indices calculated for strontianite are the result of equilibria with anhydrite, calcite, and celestite and do not indicate that strontianite is reacting in the system. As long as the waters remain saturated with these three phases, the waters could never reach saturation with strontianite, even if strontianite were present in the aquifer matrix.

In the context of inverse modeling, speciation modeling is useful because the saturation indices provide thermodynamic information about which minerals could or could not be dissolving or precipitating in a ground-water system. Thus, speciation modeling can be used to constrain the set of geochemical reactions that are possible in a regional ground-water system. However, the limitations in the interpretation of saturation indices need to be considered. Sources of uncertainty include the analytical data for the ground-water sample, the completeness and thermodynamic data of the aqueous model, and the solubility-product constants for the minerals.

Uncertainties in Speciation Models

Uncertainty in the analytical data can be minimized by careful analytical procedures (also see Chapter 6). It is possible to analyze most constituents of ground water with an accuracy of 2–5%. Similar accuracy for field measurement of alkalinity also is possible in many situations. Uncertainties of this magnitude have relatively small effects on the saturation index because saturation indices are calculated from the logs of these quantities. However, the saturation indices of some minerals (carbonate, hydroxide, and aluminous phases, among others) are strongly dependent on the value of pH; thus, uncertainties in pH can cause large uncertainties in the saturation indices for these minerals.

Uncertainties in redox parameters also can produce very large uncertainties in saturation indices. Conceptually, speciation models must have a value of the redox potential, pE, whenever it is necessary to calculate the distribution of aqueous species from an analysis of the total concentration of a redox-active element; that is, when the concentrations of individual valence states of the element have not been measured. The pE may be derived from a platinum electrode measurement or from measurements of two valence states of a redox active element (a redox couple). These methods assume that redox equilibrium obtains between the solution and the electrode or between the two valence states of the redox

couple, and, in addition, that this measured pE applies to other redox elements. However, redox reactions are often biologically mediated, kinetically slow, and element specific; therefore, in many aquifer systems, redox reactions are not in equilibrium. Consequently, estimates of pE based on equilibrium assumptions can be very poor, which, in turn, can cause major uncertainties in saturation-index calculations. Consider the following chemical reaction and the associated saturation-index equation:

$$FeS + 4H_2O \rightarrow Fe^{2+} + SO_4^{2-} + 8H^+ + 8e^- \quad (9\text{-}5)$$

$$SI_{FeS} = \log[Fe^{2+}] + \log[SO_4^{2-}] - 8\,pH - 8\,pE - 4\log[H_2O] - \log K_{FeS} \quad (9\text{-}6)$$

If analytical data are available only for sulfate and pE (as measured with a platinum electrode, for example), then an equation similar to Eq. 9-6 must be used to calculate the saturation index for the phase FeS. Note that any errors in the pH and pE are multiplied by a factor of 8.

In general, saturation indices of minerals containing redox elements will be most meaningful if the aqueous solution has been analyzed for the same valence states of the elements that are found in the mineral. In this example, if ferrous iron and total sulfide have been measured, then a speciation model can be used to calculate the activities of Fe^{2+} and HS^-. This calculation does not rely on a value of pE because it is not necessary to distribute iron or sulfur among different redox states. The saturation index for FeS can be calculated using the following chemical reaction and the associated saturation-index equation:

$$FeS + H^+ \rightarrow Fe^{2+} + HS^- \quad (9\text{-}7)$$

$$SI_{FeS} = \log[Fe^{2+}] + \log[HS^-] + pH - \log K^*_{FeS} \quad (9\text{-}8)$$

where the asterisk indicates that the solubility-product constant is for the reaction in Eq. 9-7 (not Eq. 9-5). Equation 9-8 does not depend on pE, and errors in pH are only multiplied by 1. Thus, Eq. 9-8 will provide more reliable estimates of the saturation index of FeS than will Eq. 9-6, but it is applicable only when the appropriate redox states of iron and sulfur have been measured.

Uncertainties in ion-association models are difficult to assess because there has been very little systematic application of the models to determine how well they reproduce experimental quantities, such as mean-activity coefficient or mineral solubility, over a wide range of solution compositions. The species included in the ion-association models and their stability constants usually are drawn from literature values and often are based on experiments that consider only a small range of solution composition. Little attempt has been made to maintain overall thermodynamic consistency. Specific-interaction models have been developed with much more concern about the accurate representation of experimental thermodynamic quantities and, therefore, are much more reliable for the chemical systems for which they have been developed, especially at higher ionic strengths (>0.7).

Stability constants for minerals may be uncertain because of lack of experimental data or because the minerals in a groundwater system have not been characterized. Thermodynamic data at low temperatures (~25°C) often are difficult to obtain because of the slow rates of equilibration. Another problem arises because minerals can have a range of stability due to differences in composition. For example, the stability of ferric oxyhydroxides can range over several orders of magnitude depending on the crystal structure and the degree of hydration (Langmuir 1971).

Compounding errors cause the uncertainty in the saturation index to be dependent on the stoichiometric formula of the mineral. A larger number of ions in the mass-action equation for a mineral causes larger uncertainties in the saturation index.

For example, the mass-action equation for calcite contains only two ions—calcium and carbonate—whereas the dolomite expression contains four ions—calcium, magnesium, and two carbonates. The larger number of ions leads to a larger variance in the saturation index of dolomite than calcite.

Thus, the interpretation of saturation indices requires knowledge of the aqueous model, the mineral stability and stoichiometry, and the kinetics of reactions. For low-temperature calculations, the number of minerals for which meaningful saturation indices can be calculated is relatively small. Saturation indices usually are meaningful for carbonate, sulfate, and chloride minerals because these minerals tend to react rapidly. Saturation indices for sulfides are useful if the environment is reducing and sulfide is measured. Under conditions where ferric iron can be measured, the saturation indices of ferric oxyhydroxides are meaningful. Saturation indices also are meaningful for aluminum oxides and hydroxides (provided accurate dissolved aluminum data are available), pure silica phases, and some minerals that contain trace elements. Except for kaolinite, saturation indices for most clays, feldspars, and other aluminosilicate minerals are at best qualitative because of uncertainties in the thermodynamic data and dissolved aluminum measurements.